Phase transitions of a single polymer chain: A Wang–Landau simulation study

Mark P. Taylor,[1,a)] Wolfgang Paul,[2] and Kurt Binder[2]

[1]*Department of Physics, Hiram College, Hiram, Ohio 44234, USA*
[2]*Institut für Physik, Johannes-Gutenberg-Universität, Staudinger Weg 7, D-55099 Mainz, Germany*

A single flexible homopolymer chain can assume a variety of conformations which can be broadly classified as expanded coil, collapsed globule, and compact crystallite. Here we study transitions between these conformational states for an interaction-site polymer chain comprised of $N=128$ square-well-sphere monomers with hard-sphere diameter σ and square-well diameter $\lambda\sigma$. Wang–Landau sampling with bond-rebridging Monte Carlo moves is used to compute the density of states for this chain and both canonical and microcanonical analyses are used to identify and characterize phase transitions in this finite size system. The temperature-interaction range (i.e., T-λ) phase diagram is constructed for $\lambda \leq 1.30$. Chains assume an expanded coil conformation at high temperatures and a crystallite structure at low temperatures. For $\lambda > 1.06$ these two states are separated by an intervening collapsed globule phase and thus, with decreasing temperature a chain undergoes a continuous coil-globule (collapse) transition followed by a discontinuous globule-crystal (freezing) transition. For well diameters $\lambda < 1.06$ the collapse transition is pre-empted by the freezing transition and thus there is a direct first-order coil-crystal phase transition. These results confirm the recent prediction, based on a lattice polymer model, that a collapsed globule state is unstable with respect to a solid phase for flexible polymers with sufficiently short-range monomer-monomer interactions. © *2009 American Institute of Physics.*
[doi:10.1063/1.3227751]

I. INTRODUCTION

Polymer chain molecules can undergo significant, and in some cases cooperative, conformational changes in response to changes in local environment.[1,2] Perhaps the best known example of a large-scale conformational transition exhibited by a single polymer chain is the polymer collapse or coil-globule transition which occurs in dilute polymer-solvent systems when solvent conditions are changed from "good" to "poor."[3,4] This conformational transition occurs in a continuous fashion, displaying no coexistence between distinct "coil" and "globule" states, and thus is analogous to a second-order phase transition. The helix-coil transition found in some synthetic polymers as well as proteins and nucleic acids is another example of a continuous single-chain conformational transition. In contrast, reversible protein folding provides an example of a discontinuous single-chain conformational transition, analogous to a first-order phase transition, in which there is coexistence between a folded native state and an ensemble of unfolded denatured states.[5]

In the usual rigorous theory of phase transitions, nonanalyticities in the thermodynamic functions appear only in the thermodynamic (i.e., infinite size) limit[6] and thus, when studying such transitions using computer simulations, one must make use of finite size scaling techniques.[7] In the case of single chain molecules, even for a very high molecular weight polymer, the system is always far from the thermodynamic limit. Of course one can invoke such a limit "in

theory," and thus the polymer collapse transition is thought to be a true second-order phase transition in this limit.[2] However, for biological macromolecules such as proteins which have well defined sequences and, compared to synthetic polymers, typically small sizes, no thermodynamic limit exists. For such inherently finite size systems it is still possible to define and rigorously study phase transformations. In such cases it can be advantageous to use the microcanonical ensemble where phase changes can be identified from the curvature properties of the microcanonical entropy function.[8] While the specific details of conformational transitions in biopolymers are strongly dependent on the heteropolymer nature of these macromolecules, the more universal aspects of such transitions are perhaps best explored using the prototypical model of a simple flexible homopolymer chain.

Previous work on phase transitions of single flexible square-well (SW) and Lennard-Jones (LJ) homopolymer chains has identified both a continuous collapse and a discontinuous freezing transition.[9–13] Thus, a finite length chain displays phase behavior analogous to a bulk simple liquid, where chain collapse and freezing are akin to the gas-liquid and liquid-solid transitions, respectively. In simple liquid systems, phase behavior is known to be sensitive to the range of intermolecular interaction. In particular, systems with very short-range attractive interactions exhibit no stable liquid phase, but rather undergo a direct freezing transition from a noncondensed gas/fluid phase.[14–16] Thus one might suspect that for a sufficiently short-range interaction, a flexible chain molecule would also undergo a direct transition from the

a)Electronic mail: taylormp@hiram.edu.

131, 114907-1

expanded coil to the crystal state. However, it is not immediately obvious that this is true since chain connectivity severely limits the maximum entropy of the expanded phase (compared to the vapor phase of a simple fluid) and thus, there may be insufficient driving force to induce a direct expanded-to-crystal transition.[5]

We have recently resolved this latter question, showing that a finite length chain with sufficiently short-range interactions *does* undergo a direct transition from an expanded coil to a compact crystallite.[17] This direct freezing transition was found for SW chains with lengths $N=128$ and 256 and SW interaction range of $\lambda=1.05$. In the present work we focus on the case of $N=128$ and construct a phase diagram for chains with $\lambda \le 1.30$. This phase diagram exhibits a tricritical point near $\lambda=1.06$, where the continuous coil-globule (collapse) transition and the discontinuous globule-crystallite (freezing) transition merge into a single discontinuous coil-crystallite transition. The disappearance of the globule phase from the phase diagram of a single flexible polymer chain was first observed by Rampf *et al.*[18] for the lattice bond-fluctuation polymer model in the long chain limit. These authors predicted a similar behavior for finite length chains with interactions of a shorter range than was possible in the bond-fluctuation model[19,20] and our recent results have confirmed this prediction.

II. CHAIN MODEL AND SIMULATION METHODS

In this work we study a flexible interaction-site homopolymer chain comprised of N spherically symmetric monomers connected by "universal joints" of fixed bond length L. The monomers are sequentially labeled 1 through N and monomer i is located by the vector $\vec{r}_i$. Nonbonded monomers i and j ($|i-j|>1$), separated by the distance $r_{ij}=|\vec{r}_i-\vec{r}_j|$, interact via the SW potential

$$u(r_{ij}) = \begin{cases} \infty & 0 < r_{ij} < \sigma \\ -\varepsilon & \sigma < r_{ij} < \lambda\sigma \\ 0 & r_{ij} > \lambda\sigma, \end{cases} \quad (1)$$

where σ is the hard-sphere diameter and $\lambda\sigma$ is the SW diameter. The well depth ε sets the energy scale and can be used to define a dimensionless temperature $T^*=k_BT/\varepsilon$, where k_B is the Boltzmann constant. Here we will consider the phase behavior of a SW chain of length $N=128$ and bond length $L=\sigma$ for a range of λ values. Since we deal with an isolated chain the above potential is to be treated as an effective potential which implicitly includes the effect of solvent, although here we take this potential to be temperature independent. This chain model has a discrete potential energy spectrum given by $E_n=-n\varepsilon$, where n is the number of SW overlaps in the chain configuration, and the ground state energy of the chain will depend on the interaction range λ.

The thermodynamic properties of the above chain model can be completely determined from the single chain density of states function $g(E_n)$. This function gives the volume of configurational phase space associated with each energy state E_n and can be written (relative to the value for an ideal freely jointed chain) as[21]

$$g(E_n) = \frac{\varepsilon}{V} \int \cdots \int \prod_{k=1}^{N-1} s(r_{k,k+1})$$
$$\times \delta\left(E_n - \sum_{i<j+1}^{N} u(r_{ij})\right) d\vec{r}_1, \ldots, d\vec{r}_N, \quad (2)$$

where the distribution function $s(r)=\delta(r-L)/4\pi L^2$ imposes the fixed bond length constraint and V is the total volume accessible to the chain. Although this density of states function, and a related microcanonical partition function, can be computed exactly for short ($N\le 6$) chains,[21–23] for longer chains the required high-dimensional integrals are impractical to compute numerically and one must resort to simulation methods.

Here we construct the single chain density of states function for a flexible SW chain using the Wang–Landau (WL) algorithm.[24,25] In this approach one generates a sequence of chain conformations using a set of Monte Carlo (MC) moves; however, rather than accepting new conformations with the usual temperature dependent Metropolis criterion, one uses the following temperature independent multicanonical acceptance probability:

$$P_{\text{acc}}(a \rightarrow b) = \min\left(1, \frac{w_b g(E_a)}{w_a g(E_b)}\right), \quad (3)$$

where w_a and w_b are conformation dependent weight factors which ensure microscopic reversibility for the given MC move.[26,27] If $g(E_n)$ were known, this approach would yield a uniform exploration of all accessible energy states of the system (and thus, presumably of all configurational phase space). In the WL approach $g(E_n)$ is constructed in a dynamic and iterative fashion, where smaller scale refinements are made at each level of the iteration. Thus, at the mth level of iteration, after every attempted MC move the current $g(E_n)$ value for the resulting energy state is updated with a modification factor $f_m>1$ via $g(E_n)\rightarrow f_m g(E_n)$ and a state visitation histogram $H(E_n)$ is simultaneously updated via $H(E_n)\rightarrow H(E_n)+1$. This $H(E_n)$ histogram is periodically checked for "flatness" [i.e., each entry in $H(E_n)$ is within p percent of the overall average value of $H(E_n)$] indicating an approximate equal visitation of all states. When flatness is achieved the modification factor is reduced via $f_{m+1}=\sqrt{f_m}$, the visitation histogram is reset to zero for all states, and the $(m+1)$st level of iteration is begun. One difficulty with the application of the above algorithm to chain molecules is the possible existence of "bottlenecks" in configuration space which can lead to the generation of highly asymmetric histograms which would take a prohibitively large amount of time to relax. To overcome this problem we also monitor the $H(E_n)$ histogram for uniform growth (i.e., each entry has increased by an amount within p percent of the overall average increase since the last check) and use this as an alternate flatness criterion.

In this work we start with an initial guess of $g(E_n)=1$ for all states, take $f_0=e^1$, $p=20$, and check for flatness and uniform growth every 10^4 and 5×10^7 MC cycles, respectively. Unlike most previous applications of the WL algorithm which find that $m=20$ levels of iteration ($f_{20}-1\approx 10^{-6}$) are

sufficient for convergence (with Ref. 27 being an exception), for the present study of a continuum chain molecule we find that $m \geq 26$ ($f_{26}-1 \approx 10^{-8}$) is required to achieve convergence and in most cases we continue the simulations to $m = 30$ ($f_{30}-1 \approx 10^{-9}$). Note that in the above algorithm $g(E_n)$ grows continuously throughout the calculation and that we only obtain $g(E_n)$ up to an arbitrary multiplicative constant [which drops out in the Eq. (3) acceptance criterion]. To avoid numerical difficulties we actually compute the logarithm of $g(E_n)$ and at every flatness check we uniformly reduce all entries in the $\ln[g(E_n)]$ estimate by the current maximum entry.

In our WL simulations a single MC cycle consists of, on average, the following set of attempted moves (with moves being chosen at random):[28] $N-2$ single-bead crankshaft moves in which a randomly chosen interior site i ($1 < i < N$) is rotated through a small angle about the $(i-1)$-$(i+1)$ axis; two random end bead rotations; two reptation moves in which one of the chain ends is removed and randomly reattached at the other end of the chain; one pivot move in which a portion of the chain (i.e., sites $[1, i-1]$ or $[i+1, N]$) undergoes a three-dimensional Euler rotation about a randomly chosen pivot site i ($1 < i < N$); and N "end-bridging" moves where we select at random end site 1 (or N), identify all interior sites $i > 3$ (or $i < N-2$) within distance $2L$ of this end site, and selecting one of these at random, join sites i and 1 (or N) via removal and reinsertion (at a randomly chosen azimuthal angle) of site $i-1$ (or $i+1$). The weight factor for this later bond-bridging move is $w_a = b_a J_a$, where b_a is the number of possible bridging sites i present in state a and $J_a = 1/r_{1i}$ (or $1/r_{iN}$) is a Jacobian factor arising from the fixed bond length restriction.[26] Weight factors for the other MC moves are all unity. We have verified the WL algorithm with this MC move set for the SW chain model by direct comparison with exact results for $g(E_n)$ for short SW chains ($N \leq 6$) for a range of λ ($1.01 \leq \lambda \leq 1.9$) (Ref. 21) and by comparison with the Metropolis MC results of Zhou et al.[10] for SW chains with $N \leq 64$ and $\lambda = 1.5$. For longer chains we find the bond-bridging move to be essential in order to sample compact low energy states. Also for longer chains we find it most efficient to carry out a set of WL simulations for a set of overlapping energy windows.[18] MC moves taking the system out of the energy window are rejected with no updating of $g(E)$ or $H(E)$ (note, however, that moves resulting in a hardcore overlap are always rejected *with* updating). Results from these energy windows are joined by matching $g(E)$ values at the center of the overlap region (which typically has a width of 100ε). The quality of such joins is assessed by the smoothness of the derivative of $g(E)$. Before we begin a full WL run we carry out a preliminary run at low energies, without a low energy cutoff, to estimate the ground state energy of the chain. The $H(E)$ generated in this initial WL sampling (which is restricted to level $m = 0$ and is terminated by hand) also allows us to estimate the lowest energy that can be included in our full WL run and still allows the WL method to converge in a "reasonable" amount of time. For longer chains our lowest energy window typically extends to within a few percent of the ground state energy. Care must be taken in imposing such

TABLE I. Estimated ground state energies E_{gs} and actual minimum energies E_{min} used in WL sampling for $N=128$ SW chains with well diameter $\lambda\sigma$.

λ	$-E_{gs}/\varepsilon$ (estimated)	$-E_{min}/\varepsilon$ (WL sampling)
1.02	447	439
1.05	451	440
1.10	451	447
1.15	464	450
1.20	495	475
1.25	517	500
1.30	538	524

low energy cutoffs in $g(E)$ as the resulting low temperature thermodynamics can be strongly affected.[18,29] We discuss this issue in regard to our own results later in the paper.

III. RESULTS

A. Density of states

In Table I we give our ground state energy estimates for $N=128$ SW chains for several well diameters λ in the range $1.02 \leq \lambda \leq 1.30$. As expected, this ground state energy decreases with increasing interaction range λ.[21] We also provide in Table I the lowest energy value used in our full WL simulations for this λ. As noted above, these low energy cutoffs are determined from the $H(E)$ visitation histogram generated in our preliminary WL run. These histograms typically show a sharp dropoff beyond some low energy and we set our energy cutoff just above this dropoff point.

In Fig. 1 we show our density of states results, presented in logarithmic form relative to the density of states for energy $E=0$, as $\ln[g(E)/g(0)]$ for the λ values given in Table I. These results have been obtained using two energy windows with the ranges $E \in [0, E_{join}-50\varepsilon]$ and $[E_{join}+50\varepsilon, E_{min}]$, where E_{join} is the energy at which the results of the two windows are joined which, in most cases, is set to either -250ε or -350ε. In all cases, comparison of the derivative $d \ln g(E)/dE$ from the two windows shows a very good agreement in the neighborhood of the join point.[30] The results shown in Fig. 1 are the average from two to four independent simulations for each energy window. Note that in the
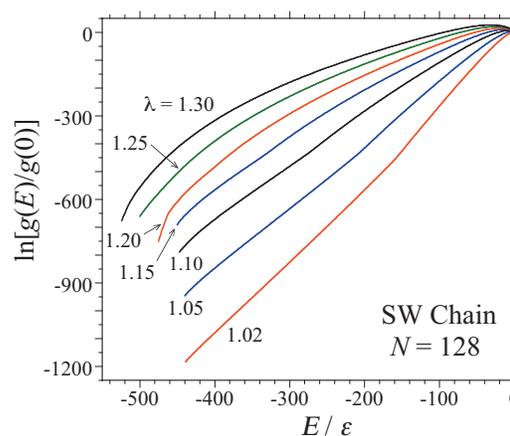

FIG. 1. Logarithm of the density of states $\ln[g(E)]$ [i.e., the microcanonical entropy $S(E)/k_B$], relative to the value at $E=0$, vs energy E for a SW chain of length $N=128$ and SW diameter $\lambda\sigma$ as indicated.

case of $\lambda=1.02$ the density of states function covers approximately 500 orders of magnitude. Although the results shown in Fig. 1 appear to be relatively featureless, these density of states functions in fact encode the complete thermodynamics of the chain molecules.[8] In Secs. III B and III C we employ a canonical and a microcanonical analysis of our $g(E_n)$ results to determine the phase behavior of the $N=128$ SW chain as a function of interaction range λ and temperature T^*. Our density of states results for these $N=128$ chains are highly reproducible although, as in Ref. 17, for smaller λ we do find some hysteresislike effects in a small energy range where crystal nucleation occurs. In all cases presented here, transition temperatures obtained from independent runs agree to within $\delta T^*=\pm 0.006$.

B. Canonical analysis

From the single chain density of states $g(E_n)$ one can construct the canonical ensemble partition function

$$Z(T) = \sum_n g(E_n)e^{-E_n/k_BT} \tag{4}$$

and the canonical probability function

$$P(E_n,T) = \frac{1}{Z(T)}g(E_n)e^{-E_n/k_BT}. \tag{5}$$

From these we obtain the Helmholtz free energy

$$F(T) = -k_BT \ln Z(T) \tag{6}$$

and the internal energy

$$U(T) = \langle E_n \rangle = \sum_n E_n P(E_n,T). \tag{7}$$

Since the WL simulation method only gives $g(E_n)$ up to an arbitrary multiplicative constant, we only know $F(T)$ up to an arbitrary additive linear function of T. However, the internal energy and other averages over functions of E_n are determined absolutely. To locate phase transitions within the canonical ensemble one typically examines the specific heat function

$$C(T) = \frac{dU}{dT} = \frac{1}{k_BT^2}(\langle E_n^2 \rangle - \langle E_n \rangle^2). \tag{8}$$

For a finite size system, maxima in $C(T)$ can be associated with phase transitions or other structural rearrangements.[9,10,27] A first-order transition can be identified by a bimodal $P(E_n,T)$ probability distribution with equal weight in the peaks which correspond to the two coexisting states.

In Fig. 2 we show the canonical specific heat $C(T)$ obtained from our density of states results for a range of well diameters λ. For larger values of λ [$\lambda \geq 1.15$, shown in Fig. 2(b)] these curves all display a high temperature peak and broad plateau followed (with the exception of $\lambda=1.30$) by a stronger low temperature peak. As λ is decreased, these two peaks increase in height and the plateau region narrows, with the high temperature peak moving to lower T and the low temperature peak moving to higher T. We can identify the high temperature peak with the chain collapse or coil-globule
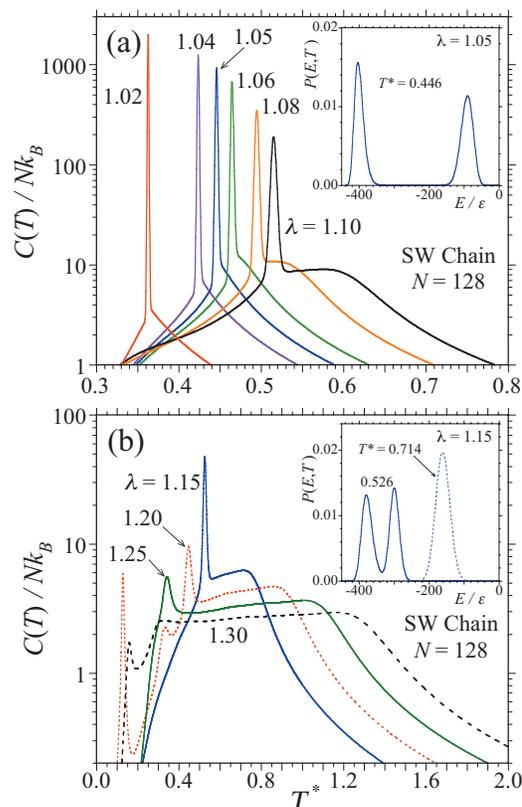

FIG. 2. Specific heat per monomer $C(T)/Nk_B$ vs temperature T^* for a SW chain of length $N=128$ and SW diameter $\lambda\sigma$ as indicated for (a) $\lambda \leq 1.10$ and (b) $\lambda \geq 1.15$. Insets: canonical probability function $P(E,T)$ vs energy E for (a) $\lambda=1.05$ and (b) $\lambda=1.15$ at the indicated temperatures T^*, which correspond to the peaks in the associated $C(T)$ curve. Solid curves show the equally weighted bimodal distributions characterizing a first-order transition and the dashed curve for $\lambda=1.15$ shows the distribution at the continuous coil-globule transition.

transition and the low temperature peak with the chain freezing transition.[9–12] (The absence of a freezing peak in the case of $\lambda=1.30$ will be further discussed below). The inset in Fig. 2(b) shows that for $\lambda=1.15$ the collapse and freezing transitions are characterized, respectively, by unimodal and bimodal $P(E,T)$ probability distributions. Thus we have a continuous chain collapse transition followed by a discontinuous chain freezing transition. With increasing λ the freezing transition weakens, with the two peaks of the bimodal $P(E,T)$ distribution merging, leading to a unimodal probability distribution at "freezing" for $\lambda=1.25$ and no clear freezing peak in $C(T)$ for $\lambda=1.30$. In the following sections we will make use of a microcanonical analysis to further characterize the low temperature behavior of these chains with larger λ.

For SW diameters less than $\lambda=1.10$, shown in Fig. 2(a), the $C(T)$ curves undergo an interesting change in structure. The collapse-peak plateau becomes a shoulder for $1.06 \leq \lambda \leq 1.08$ and then disappears for $\lambda \leq 1.05$ leaving a very narrow spike at the freezing transition. The $P(E,T)$ probability distribution for $\lambda=1.05$ at the freezing temperature, shown in the inset of Fig. 2(a), is strongly bimodal with two very well separated peaks. Thus for a sufficiently short-range monomer-monomer interaction the $N=128$ SW chain undergoes a very strong first-order freezing transition directly from a high-energy (and, as shown below, expanded) state.[17]

These results suggest the disappearance of a distinct chain collapse transition for chains with short-range interactions as predicted by Paul and co-workers[19,20] and discussed in Sec. I. In the next section we focus on this issue using an alternate, microcanonical thermodynamic analysis.

C. Microcanonical analysis

A weakness of the above canonical analysis is the inability to definitely locate the disappearance of the collapse transition since the specific heat collapse peak smoothly merges into the freezing peak. However, as we have recently shown,[17] it is possible to clearly distinguish the collapse and freezing transitions via analysis within the microcanonical ensemble. Such an analysis is based on the curvature of the microcanonical entropy function

$$S(E) = k_B \ln g(E) \qquad (9)$$

(shown in Fig. 1) and has proven very useful in studying phase transitions in finite size systems.[8,31–33]

Discontinuous or first-order phase transitions are particularly distinct in the microcanonical analysis, being signaled by a so-called "convex intruder" in $S(E)$. This feature results in a characteristic Maxwell-type loop in the microcanonical temperature given by

$$T(E) = [dS/dE]^{-1}. \qquad (10)$$

The coexisting states and transition temperature for this discontinuous transition can be obtained from either a common tangent construction on the $S(E)$ curve or via an equal area construction on the $T^{-1}(E)$ curve (also known as the inverse caloric curve). A continuous phase transition is signaled by the existence of an isolated inflection point (which becomes a saddle point in the thermodynamic limit) in $T(E)$. In a finite system such a point will produce a finite peak in the microcanonical specific heat given by

$$c(E) = [dT/dE]^{-1} = \frac{-1}{T^2(E)} \left(\frac{d^2 S}{dE^2} \right)^{-1}. \qquad (11)$$

For a first-order phase transition, the loop in the $T(E)$ caloric curve produces a very distinct signature in this specific heat function, consisting of a negative region bounded by two poles (where $dT(E)/dE=0$), demarking an energy region which is thermally unstable.

In Fig. 3 we show an example of this microcanonical analysis for the case of $\lambda=1.15$. The inverse caloric curve $T^{-1}(E)$, shown in the main figure, is used to locate discontinuous transitions and the microcanonical specific heat $c(E)$, shown in the inset, is used to locate continuous transitions. The clear Maxwell-type loop in $T^{-1}(E)$ [and the associated poles in $c(E)$] indicates the discontinuous freezing transition and an equal area construction across this loop finds the coexisting energy states to be $-E/\varepsilon=299(1)$ and $379(1)$ at a transition temperature of $T^*=0.526(1)$. The weak isolated peak in $c(E)$ indicates the continuous coil-globule transition, which is located at energy $-E/\varepsilon=158(4)$, which corresponds to temperature $T^*=0.718(4)$. These microcanonical transition temperatures are in agreement with the results obtained from the previous canonical analysis, where the freezing and col-
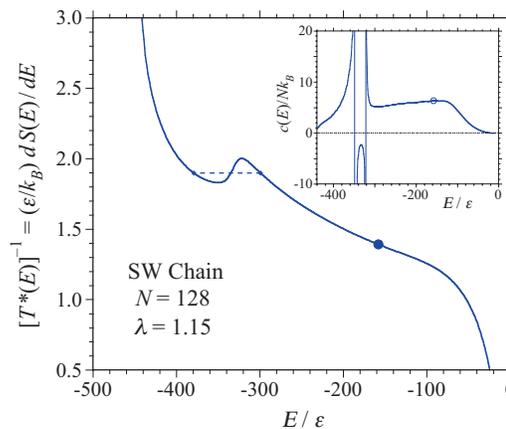

FIG. 3. Derivative of the microcanonical entropy for $N=128$, $\lambda=1.15$. The dashed tie line, obtained by an equal area construction, locates the transition temperature and coexisting states for the first-order freezing transition. The filled circle at $E=-158\varepsilon$ locates the continuous coil-globule transition. Inset: microcanonical specific heat $c(E)$ vs energy E. The isolated peak, marked by the open circle, locates the coil-globule transition energy.

lapse peaks in the canonical specific heat function $C(T)$, shown in Fig. 2(b) for $\lambda=1.15$, are located at $T^*=0.526(1)$ and $0.714(2)$, respectively.

The usefulness of the microcanonical analysis is made evident in Fig. 4 where we show the inverse caloric curves for three cases in which the canonical analysis is unable to definitely locate a coil-globule transition due to the merging of the collapse and freezing specific heat peaks [see Fig. 2(a)]. Each curve in Fig. 4 shows a very pronounced Maxwell-type loop indicating a strong first-order transition. Equal area constructions on these loops, marked by the dashed tie lines, give the temperatures and coexisting energy states at the transition. In addition to a first-order freezing transition, for each case shown in Fig. 4 there is also a continuous transition signaled by an inflection point in $T(E)$ [or equivalently by an isolated peak in $c(E)$] and indicated by the filled circles. In the case of $\lambda=1.05$ this continuous tran-
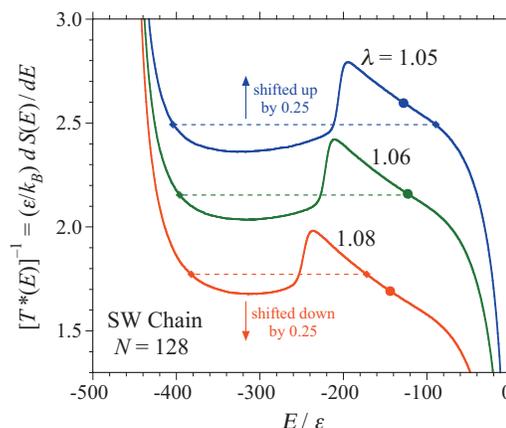

FIG. 4. Derivative of the microcanonical entropy for $N=128$, $\lambda=1.05$, 1.06, and 1.08, as indicated, vs energy E. As in Fig. 3, the dashed tie lines locate the transition temperatures and coexisting states for the first-order freezing transition and the filled circles locate the continuous coil-globule transition (with uncertainty being indicated by the symbol sizes). For $\lambda=1.05$, the latter transition is seen to fall within the freezing transition coexistence region. Note that the curves for $\lambda=1.05$ and 1.08 have been shifted for clarity.
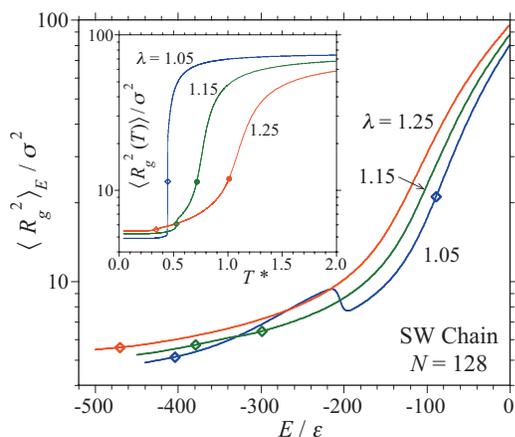
FIG. 5. Microcanonical mean square radius of gyration $\langle R_g^2 \rangle_E$ vs energy E for $N=128$ with $\lambda=1.05$, 1.15, and 1.25 as indicated. Inset: canonical mean square radius of gyration $\langle R_g^2(T) \rangle$ vs reduced temperature T^*. The filled circles and open diamonds locate the collapse and freezing transitions, respectively.
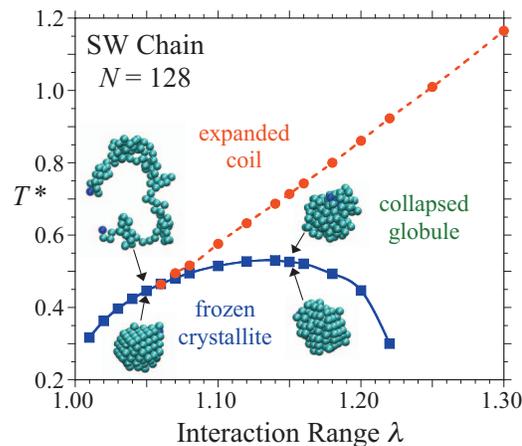

FIG. 6. Temperature-interaction range (T-λ) phase diagram for the $N=128$ SW chain. The filled circles locate the continuous coil-globule (collapse) transition and the filled squares locate the discontinuous globule-crystal or coil-crystal freezing transition. The connecting dashed and solid lines are simply interpolations between these points and uncertainties are smaller than the symbol size. The simulation snapshots show representative chain conformations coexisting at the freezing transition for interaction ranges $\lambda=1.05$ ($-E/\varepsilon=404$ and 89) and $\lambda=1.15$ ($-E/\varepsilon=379$ and 299), as indicated. For short-range interactions ($\lambda \leq 1.05$) the chain freezes directly from an expanded coil state while for longer range interactions ($\lambda > 1.06$) the chain freezes from the collapsed globule state.

sition is seen to be located *within* the coexistence region of the freezing transition. Thus, for this short-range interaction the continuous collapse transition is pre-empted by the freezing transition and there is a direct coil-crystallite transition. For the case of $\lambda=1.06$ the collapse transition essentially coincides with the onset of the coexistence region while for larger λ the collapse transition energy clearly moves outside the coexistence energy range. Thus for $\lambda > 1.06$ there are distinct collapse and freezing transitions.

D. Chain dimensions and structure

In our above analysis of phase transitions of a single polymer chain we have assumed that the high temperature (high energy) continuous transition corresponds to chain collapse and the low temperature (low energy) discontinuous transition corresponds to chain freezing. To verify the nature of these transitions we have carried out additional structural analysis, computing average chain dimensions and examining configurational snapshots.

To both compute chain dimensions and generate typical equilibrium configurations we carry out a multicanonical-type simulation,[34] using the acceptance probability given by Eq. (3), with fixed $g(E)$ given by the final results of our WL simulations. In the course of this simulation we determine the microcanonical mean-square radius of gyration

$$\langle R_g^2 \rangle_E = \frac{1}{N^2} \sum_{i<j}^{N} \langle r_{ij}^2 \rangle_E, \tag{12}$$

where the angular brackets indicate an average over chain conformations with energy E. The mean-square radius of gyration at canonical temperature T is then simply given by

$$\langle R_g^2(T) \rangle = \sum_E \langle R_g^2 \rangle_E P(E,T), \tag{13}$$

where the canonical probability distribution $P(E,T)$ is given by Eq. (5). Both canonical and microcanonical radius of gyration results are shown in Fig. 5 for $N=128$ SW chains with SW diameters $\lambda=1.05$, 1.15, and 1.25. For the two larger

well diameters the microcanonical radius of gyration decreases monotonically with decreasing energy and there are no clear signals in chain size itself indicating a phase transition. For the shorter range interaction ($\lambda=1.05$), the chain exhibits a surprising abrupt increase in average size as the energy decreases near $-E/\varepsilon \approx 200$. This step in $\langle R_g^2 \rangle_E$ occurs within the two-phase region and coincides with the location of the free energy $[F(E,T)=-\ln P(E,T)=E-TS(E)]$ barrier separating the coexisting coil and crystallite states (which also approximately coincides with the upper energy bound of the thermally unstable region).[17] An analysis of conformational snapshots at $-E/\varepsilon \approx 210$ shows that this local maximum in chain size is due to the formation of a transition state structure consisting of a crystalline nucleus attached to one or more extended chain segments.

In the inset of Fig. 5 we show the canonical mean-square radius of gyration as a function of temperature. These curves all display the usual sigmoidal shape expected for the chain collapse transition[2] and the filled circles indicate the collapse transition temperatures for $\lambda=1.15$ and 1.25. For $\lambda=1.15$ the lower temperature freezing transition is evident as a small step in $\langle R_g^2(T) \rangle$ at the freezing temperature. A much larger step is seen for the case of $\lambda=1.05$ where there is a direct freezing transition from the coil state (i.e., there is no separate collapse transition). The open diamonds in the Fig. 5 inset locate the freezing transition temperature, which is seen to fall approximately in the middle of steps in $\langle R_g^2(T) \rangle$. For $\lambda=1.25$ the energy discontinuity at freezing is very small (or, as discussed below, zero) and there is no apparent step in $\langle R_g^2(T) \rangle$.

Representative chain conformations at the freezing transition are shown within Fig. 6 for the cases of $\lambda=1.05$ and 1.15. These simulation snapshots are of conformations with sizes approximately equal to the average chain sizes for the

TABLE II. Freezing and coil-globule transition temperatures for $N=128$ SW chains with well diameter $\lambda\sigma$. The numbers in parentheses are the estimated uncertainty in the last digit shown. Freezing temperatures in square brackets correspond to cases where there is no clear Maxwell loop in $T(E)$ associated with the freezing peak in $C(T)$.

λ	T_f^*	T_{c-g}^*
1.01	0.317(3)	…
1.02	0.363(2)	…
1.03	0.397(1)	…
1.04	0.424(1)	…
1.05	0.446(1)	0.426(2)
1.06	0.465(1)	0.463(4)
1.07	0.481(1)	0.495(3)
1.08	0.495(1)	0.516(2)
1.10	0.515(1)	0.576(1)
1.12	0.527(1)	0.633(1)
1.14	0.530(1)	0.687(1)
1.15	0.526(1)	0.714(2)
1.16	0.521(1)	0.743(2)
1.18	0.493(4)	0.800(2)
1.20	0.447(4)	0.861(2)
1.22	[0.300(4)]	0.923(2)
1.25	[0.342(6)]	1.010(5)
1.30	?	1.165(5)

coexisting energy states at freezing (as indicated in Fig. 5). These energies are given by the tie-line analysis shown in Figs. 3 and 4 and also correspond to the most probable energies at freezing, given by the peaks in $P(E,T)$ shown in the Fig. 2 insets. For $\lambda=1.05$ a well-ordered crystallite coexists with a disordered expanded coil, while for $\lambda=1.15$ a somewhat less ordered crystallite coexists with a disordered compact globule. In general, a single snapshot is insufficient to summarize the large number of conformations sampled by a flexible chain at any energy. However, both visual examination and analysis of pair probability functions for a large number of independent chain conformations at each of the coexistence energies confirm that these snapshots are quite representative of the ensemble of structures at that energy. We also note that with increasing well diameter the degree of order in the coexisting crystallite state clearly decreases.

E. Single chain phase diagram

Combining our canonical and microcanonical calorimetric results, which precisely locate phase transitions, with our direct structural analysis of these phases, we are able to build a phase diagram for the single flexible polymer chain. In Fig. 6 we show the temperature-interaction range (T-λ) phase diagram for the $N=128$ SW chain for $1.01\leq\lambda\leq1.30$ constructed from the transition temperatures given in Table II. For $\lambda>1.06$ the high temperature expanded coil phase is separated from the low temperature crystallite phase by an intervening collapsed globule phase. Thus, upon cooling, an expanded chain undergoes a continuous coil-globule (collapse) transition followed by a discontinuous globule-crystallite (freezing) transition. For $\lambda<1.06$ the collapsed globule state is no longer thermodynamically stable and there is a direct freezing transition from the expanded coil to the crystallite phase. Thus, as predicted by Paul and

co-workers,[19,20] the phase diagram for a single flexible polymer chain contains a tricritical point where the continuous coil-globule transition and the discontinuous globule-crystal transition merge into a single discontinuous coil-crystal transition. For the $N=128$ SW chain this tricritical point is located at approximately $\lambda\approx1.06$, $T^*\approx0.465$.

In the Fig. 6 phase diagram we have terminated the freezing line at $\lambda=1.22$ because the exact nature and location of the freezing transition for larger interaction range are not clear. In fact, the Maxwell-type loop signaling the discontinuous freezing transition is not present in our results for $1.22\leq\lambda\leq1.45$ (although in all of these cases we have a well defined saddle point or nearly flat plateau in lieu of a loop). This difficulty in clearly identifying the freezing transition from our density of states results may be due, in part, to our cutoff of the lowest energy states in our WL sampling. It is known that low energy cutoffs can lead to incorrect low temperature thermodynamic results[29] and the WL results of Parsons and Williams[35] appear to miss the freezing transition of a LJ chain due to such an inappropriate energy cutoff. Alternatively, there may in fact be no true freezing (i.e., discontinuous ordering) transition for $N=128$ SW chains with $1.22\leq\lambda\leq1.45$, although our $C(T)$ results do suggest some type of weak transition in the vicinity where we expect freezing. In the case of a simple monomeric SW liquid there is evidence that there is *no* freezing transition in the case of $\lambda=1.40$ and that the freezing temperature is strongly suppressed for slightly larger well diameters.[36] Thus, we may be seeing a reflection of this bulk fluid behavior in our finite length chains, but occurring for somewhat smaller well diameter. We do find a discontinuous freezing transition for $\lambda=1.50$ in agreement with the earlier findings of Zhou *et al.*[10] and we note that these authors were similarly unable to find evidence of a discontinuous freezing transition for their SW chain model with $N=64$ and $\lambda=1.30$.

IV. DISCUSSION

In this work we have examined conformational transitions of a single polymer chain and constructed the temperature-interaction range phase diagram for a SW chain with length $N=128$. This phase diagram is comprised of regions of expanded coil, collapsed globule, and compact crystallite structures. For interaction ranges $\lambda>1.06$ there is a continuous coil-globule (collapse) transition at a temperature somewhat lower than the SW monomer Boyle temperature (defined below) and a discontinuous globule-crystallite (freezing) transition at lower temperature. For $\lambda\leq1.05$ a microcanonical analysis unambiguously shows that the collapse transition is pre-empted by the freezing transition and there is a direct transition from an expanded coil to a compact crystallite. Thus the SW chain phase diagram contains a tricritical point where the continuous collapse and discontinuous freezing transitions merge into a single discontinuous coil-crystallite transition. These findings confirm the recent predictions of Paul *et al.*[19] regarding the disappearance of the globule phase for flexible chain molecules with sufficiently short-range interactions and our Fig. 5 phase diagram has the topology proposed by Binder and Paul.[20] The phase behavior

of the finite SW chain is thus similar to that of a monomeric SW fluid for which the gas-liquid condensation transition is pre-empted by a gas-solid freezing transition when $\lambda \lesssim 1.25$ resulting in the loss of a stable liquid phase.[16] This absence of a stable liquid phase is a general feature of simple liquids (or colloids) with very short-range interactions.[14,15]

The results presented here have been restricted to a polymer chain of length $N=128$. Although such modest length chains are relevant to the study of small proteins, for many other applications it will be of interest to extend our results to longer chains. For example, as has been pointed out previously, the phase behavior of a single long polymer chain can be mapped onto that of a polymer solution[19,20] and thus our single chain results may provide insight into the behavior of a many chain system. Thus, in addition to our rather extensive set of simulations for SW chains with $N=128$, we have also carried out a smaller set of simulations for SW chains of lengths $N=32$, 64, and 256. These data have allowed us to make a preliminary finite size scaling analysis of the SW chain phase behavior. In general, it is observed that with increasing length the SW chain collapse and freezing transitions systematically move to higher temperatures, similar to the scaling behavior previously reported for the lattice bond-fluctuation chain model.[18,19] In the $N \rightarrow \infty$ long chain limit the SW chain tricritical point moves to $\lambda \approx 1.15$, T^* ≈ 0.85 and (for all $\lambda > 1.15$) the coil-globule transition temperature moves very close to the SW monomer Boyle temperature T_B^*, given by

$$1/T_B^* = -\ln(1 - 1/\lambda^3). \tag{14}$$

A complete scaling analysis of the flexible SW chain will be the subject of a future publication.

One interesting observation made in the present study is that the progress of the WL simulation itself can reveal information about transition pathways in the system. In particular, in all cases in which we find a discontinuous freezing transition we have observed a configurational barrier within the WL simulation. That is, as the simulation proceeds there is a thorough exploration of the set of energy states above and below a narrow band of "barrier" states, but crossing of this barrier is a rare event. This type of dynamics is also observed in our multicanonical simulations, which are run using our converged $g(E)$ functions, and has been previously discussed by Neuhaus and Hager[37] in the context of condensation and freezing in the two-dimensional (2D) Ising model. As noted above, the observed configurational barrier appears to be associated with a nucleation event, characteristic of a first-order phase transition, leading to the formation of a partially crystalline transition state structure. Interestingly, this type of configurational barrier is also observed in those cases where we expect, but do not find a discontinuous freezing transition [i.e., no Maxwell loop in $T(E)$]. Such behavior is found for $1.25 \lesssim \lambda \lesssim 1.45$ where we see a very pronounced inflection point in $T(E)$, indicating a continuous transition, in the energy range where we would have expected a Maxwell loop associated with a discontinuous globule-crystallite freezing transition. The existence of a configurational barrier in these cases suggests that we may actually have phase coexistence between two distinct populations of structures, one

ordered and the other disordered, but both at the same energy. In order to further elucidate this configurational barrier we plan to carry out additional multicanonical simulations using our WL $g(E)$ functions to construct 2D free energy landscapes that depend on both the energy E and either average chain size $\langle R_g^2 \rangle_E$ or a local order parameter Q. We may also attempt to carry out 2D WL simulations to construct joint density of states functions[38,39] such as $g(E,\lambda)$, $g(E,\langle R_g^2 \rangle_E)$, or $g(E,Q)$. Adding a dimension to the WL sampling is known to allow for easier movement through configuration space, providing alternate pathways around barriers.

Although the full nature of globule-crystallite freezing transition requires further characterization, the direct coil-crystallite freezing transition of the SW chain found for $\lambda \lesssim 1.05$ is clearly discontinuous and provides an interesting example of phase coexistence in a finite size system. The transition is characterized not only by coexistence between the expanded coil and compact crystallite structures, but at the transition state itself there is an apparent coexistence within the single chain between a crystal nucleus domain and one or more extended disordered chain sections.

The crystal structure of the frozen SW chain has not yet been completely determined, although we have established that for the short-range interactions ($\lambda \lesssim 1.05$) the chains freeze into a crystallite (with defects and grain boundaries) with hexagonal-close-packed (hcp) structure and this structure persists (becoming more uniform) down to the ground state energy. In contrast, in the case of a bulk SW monomer system with short-range interactions, the ground state is thought to have a face-centered-cubic (fcc) structure[36] and for $\lambda \lesssim 1.05$ the system undergoes a solid-solid transition at high pressures.[40] For somewhat longer range interactions the solid-state phase behavior of the bulk SW system is even more complex, being λ dependent and including numerous solid-solid transitions.[36,41,42] While one cannot make direct comparison between the phase behavior of the bulk SW monomer system and an isolated (i.e., in vacuum) finite length SW polymer chain, one might expect that the phase behavior of a long single chain will be similar to that of the bulk system at low pressures. The solid-state phase behavior of the bulk SW monomer system has been particularly well studied for the two well diameters $\lambda=1.50$ (Ref. 41) and 1.43.[42] For the $\lambda=1.50$ SW system at low pressures the initial freezing transition is into a hcp structure and upon further cooling the system undergoes a hcp-fcc solid-solid transition. For the $\lambda=1.43$ SW system at low pressure the initial freezing transition is into a body-centered-cubic (bcc) phase followed by a lower temperature bcc-hcp solid-solid phase transition. These results suggest that a solid-solid transition may also occur in the SW chain. There is evidence for this in the case of $\lambda=1.20$ where the presence of a second low temperature peak in $C(T)$ [Fig. 2(b)] and the pronounced low energy kink in $S(E)$ [Fig. 1] may indeed indicate such a transition. We find a similar second low temperature peak in $C(T)$ for $\lambda=1.18$ but not for $\lambda=1.22$. Alternatively, these additional low temperature peaks in $C(T)$ may be due to simple excitations from the ground state structure rather than

global structural transformations.[27] A more detailed analysis of the crystal structure and solid-state phase behavior of the SW chains are currently being pursued.

ACKNOWLEDGMENTS

[1] P. J. Flory, *Principles of Polymer Chemistry* (Cornell University Press, Ithaca, 1953).

[2] A. Yu. Grosberg and A. R. Khokhlov, *Statistical Physics of Macromolecules* (AIP, New York, 1994).

[3] W. H. Stockmayer, Macromol. Chem. Phys. **35**, 54 (1960).

[4] I. Nishio, S.-T. Sun, G. Swislow, and T. Tanaka, Nature (London) **281**, 208 (1979); G. Swislow, S.-T. Sun, I. Nishio, and T. Tanaka, Phys. Rev. Lett. **44**, 796 (1980).

[5] A. V. Finkelstein and O. B. Ptitsyn, *Protein Physics* (Academic, New York, 2002).

[6] R. K. Pathria, *Statistical Mechanics* (Pergamon, New York, 1985).

[7] K. Binder and D. W. Heermann, *Monte Carlo Simulations in Statistical Physics* (Springer, New York, 1997).

[8] D. H. E. Gross, *Microcanonical Thermodynamics* (World Scientific, Singapore, 2001).

[9] Y. Zhou, C. K. Hall, and M. Karplus, Phys. Rev. Lett. **77**, 2822 (1996).

[10] Y. Zhou, M. Karplus, J. M. Wichert, and C. K. Hall, J. Chem. Phys. **107**, 10691 (1997).

[11] H. Liang and H. Chen, J. Chem. Phys. **113**, 4469 (2000).

[12] M. P. Taylor, J. Chem. Phys. **114**, 6472 (2001).

[13] F. Calvo, J. P. K. Doye, and D. J. Wales, J. Chem. Phys. **116**, 2642 (2002).

[14] A. P. Gast, C. K. Hall, and W. B. Russel, J. Colloid Interface Sci. **96**, 251 (1983).

[15] M. H. J. Hagen and D. Frenkel, J. Chem. Phys. **101**, 4093 (1994).

[16] D. L. Pagan and J. D. Gunton, J. Chem. Phys. **122**, 184515 (2005); H. Liu, S. Garde, and S. Kumar, *ibid.* **123**, 174505 (2005).

[17] M. P. Taylor, W. Paul, and K. Binder, Phys. Rev. E **79**, 050801(R) (2009).

[18] F. Rampf, W. Paul, and K. Binder, Europhys. Lett. **70**, 628 (2005); F. Rampf, K. Binder, and W. Paul, J. Polym. Sci., Part B: Polym. Phys. **44**, 2542 (2006).

[19] W. Paul, T. Strauch, F. Rampf, and K. Binder, Phys. Rev. E **75**, 060801(R) (2007).

[20] K. Binder and W. Paul, Macromolecules **41**, 4537 (2008).

[21] M. P. Taylor, J. Chem. Phys. **118**, 883 (2003).

[22] J. E. Magee, L. Lue, and R. A. Curtis, Phys. Rev. E **78**, 031803 (2008).

[23] M. P. Taylor, K. Isik, and J. Luettmer-Strathmann, Phys. Rev. E **78**, 051805 (2008).

[24] F. Wang and D. P. Landau, Phys. Rev. Lett. **86**, 2050 (2001); Phys. Rev. E **64**, 056101 (2001).

[25] D. P. Landau, S.-H. Tsai, and M. Exler, Am. J. Phys. **72**, 1294 (2004).

[26] F. A. Escobedo and J. J. de Pablo, J. Chem. Phys. **102**, 2636 (1995).

[27] T. Wüst and D. P. Landau, Phys. Rev. Lett. **102**, 178101 (2009).

[28] D. P. Landau and K. Binder, *Monte Carlo Simulations in Statistical Physics* (Cambridge University Press, Cambridge, 2000).

[29] D. T. Seaton, S. J. Mitchell, and D. P. Landau, Braz. J. Phys. **38**, 48 (2008).

[30] More generally we find a very good agreement in $d \ln g(E)/dE$ across the entire overlap region with the exception of the extreme upper edge, where this derivative in the low energy window is clearly distorted.

[31] C. Junghans, M. Bachmann, and W. Janke, Phys. Rev. Lett. **97**, 218103 (2006).

[32] W. Paul, F. Rampf, T. Strauch, and K. Binder, Comput. Phys. Commun. **179**, 17 (2008).

[33] J. Hernandez-Rojas and J. M. Gomez Llorente, Phys. Rev. Lett. **100**, 258104 (2008).

[34] A. Mitsutake, Y. Sugita, and Y. Okamoto, Biopolymers **60**, 96 (2001).

[35] D. F. Parsons and D. R. M. Williams, J. Chem. Phys. **124**, 221103 (2006); Phys. Rev. E **74**, 041804 (2006).

[36] E. Velasco, P. Tarazona, M. Reinaldo-Falagan, and E. Chacon, J. Chem. Phys. **117**, 10777 (2002).

[37] T. Neuhaus and J. S. Hager, J. Stat. Phys. **113**, 47 (2003).

[38] C. Zhou, T. C. Schulthess, S. Torbrügge, and D. P. Landau, Phys. Rev. Lett. **96**, 120201 (2006).

[39] J. Luettmer-Strathmann, F. Rampf, W. Paul, and K. Binder, J. Chem. Phys. **128**, 064903 (2008).

[40] P. Bolhuis, M. Hagen, and D. Frenkel, Phys. Rev. E **50**, 4880 (1994).

[41] D. A. Young and B. J. Alder, J. Chem. Phys. **73**, 2430 (1980).

[42] J. Serrano-Illan, G. Navascues, and E. Velasco, Phys. Rev. E **73**, 011110 (2006).